https://doi.org/10.3311/PPee.38682

Periodica Polytechnica Electrical Engineering and Computer Science, 69(1), pp. 43–52, 2025

Formation Control Design of Fixed-wing UAVs Based on Model Reference Adaptive Control

Bela Lantos[1], Stephen Kimathi[1,2*]

[1] Department of Control Engineering and Information Technology, Faculty of Electrical Engineering and Informatics, Budapest University of Technology and Economics, Műegyetem rkp. 3., H-1111 Budapest, Hungary
[2] Department of Electrical and Electronic Engineering, Dedan Kimathi University of Technology, P.O.B. 10143, 10100 Dedan Kimathi, Nyeri, Kenya
* Corresponding author, e-mail: kimathi@iit.bme.hu

Received: 29 October 2024, Accepted: 06 December 2024, Published online: 06 January 2025

Abstract

Formation control is currently a popular field of research due to the increasing application areas of unmanned aerial vehicles. Of concern is the stability of unmanned aerial vehicles (UAVs) formation while tracking especially under the influence of disturbances, and model parameter uncertainty. Since formation of the UAV formation while tracking, especially flying involves a mutual cooperation, consensus-based techniques are more suited such that a group of UAVs are collectively coordinated to perform some tasks. In this paper, a leader–follower formation control of homogeneous fixed wing UAVs based on model reference adaptive control with an integral error control compensation is presented. Model reference adaptive control is powerful and effective for handling uncertain and varying dynamics. This proposed distributed composite control strategy with a directed graph topology, although model-dependent can be effective to suppress disturbances affecting the vehicles, while achieving consensus-based tracking of a reference path. The numerical simulation results given show the applicability of this proposed control strategy.

Keywords

adaptive control, nominal control, stability tuning, parameter tuning, leader-follower formation, fixed-wing UAVs

1 Introduction

Formation control involves the design of algorithms to coordinate a group of agents to form, and maintain prescribed shapes and patterns, while in motion [1]. Complexity challenges associated with formation control of multi-agent systems include nonlinear dynamics, model parameter variations, and the presence of external disturbances in the system dynamics. Several solutions have been presented in the literature to solve these challenges including the use of adaptive control [2, 3], disturbance observers [4], robust control [5] and neural networks [6].

Model reference adaptive control was presented for the cooperative tracking of uncertain dynamical multi-agent systems in [7, 8], for aerial vehicles in [2, 9], and for vehicle platoons in [10]. Distributed control methods have been applied in [11, 12] for state synchronization of multiple vehicles, and in [13] for the tracking control of unmanned aerial vehicles (UAVs) under external disturbances. Other distributed control techniques include predictive control in [14, 15], application of neural networks in [16, 17], and a multivariable adaptive control in [18], where it was shown that adaptive control was effective in handling uncertain dynamic parameters.

For a single UAV, its prescribed velocity must be the tangential of a designed path [10], where the position, velocity and acceleration models are considered. In such a situation, therefore, an acceleration level control is designed which in effect transforms the kinematics into double integrator dynamics which is unstable. Hence, the system must be stabilized by state feedback, and with the assumption that consensus-based formation is similar to a one-step ahead predictive control problem, due to the reliance on the neighboring vehicles' state information, this necessitates the interaction of the vehicles to be modelled using a directed graph topology [19].

The adaptive formation control such as that discussed in [2, 3], presents a leader-follower formation configuration of homogenous UAVs, modelled using a directed graph. And on the basis of adaptive tuning of gains, the control laws do not require global states, but rather relative

Cite this article as: Lantos, B., Kimathi, S. "Formation Control Design of Fixed-wing UAVs Based on Model Reference Adaptive Control", Periodica Polytechnica Electrical Engineering and Computer Science, 69(1), pp. 43–52, 2025. https://doi.org/10.3311/PPee.38682

information of the neighbors' states. In our work, model reference adaptive control method is applied due to its versatility, and with a well-defined formation error and use of integral control, we show that it is effective in maintaining and suppressing disturbances and errors in a formation system. Due to the adaptive tuning of gains, we show that the proposed control strategy guarantees the boundedness of control signals, and system states under the presence of model parameter uncertainty and disturbances on the vehicles. The main novelties are that the formation control is consensus-based, and the model perturbations and disturbance compensation approach presented, is easy and consistent, such that the flexibility of activating different adaptation components is shown.

The structure of the paper is as follows: Section 2 deals with modeling and control of a single UAV where the simple control using pole placement is used to stabilize the double integrator dynamics. Section 3 discusses some principles related to the stability and parameter tuning in UAV formations using adaptive control, and the distributed adaptive control algorithm is presented in Section 4. Section 5 presents the numerical simulation results, and the conclusions are given in Section 6.

2 Modeling and control of a single UAV

For a single UAV, the position $p \in \mathbb{R}^3$, velocity $v \in \mathbb{R}^3$ and acceleration $a \in \mathbb{R}^3$ are considered. The velocity vector v having a magnitude $V = \|v\|$ is assumed tangential to the direction of motion. The angle between the velocity vector and the horizontal direction is chosen as γ, and the portion $V\cos(\gamma)$ is projected onto the horizontal plane such that the components in $x - y$ directions can be found by a rotation ψ about the z axis, see [20]. With this description, the point-mass equations governing motion of a fixed wing UAV can be postulated.

2.1 Kinematic equations

Assuming a flat and stationary earth, the model dynamics can be described using:

$$\begin{aligned} \dot{x} &= V\cos(\gamma)\cos(\psi) + d_x \\ \dot{y} &= V\cos(\gamma)\sin(\psi) + d_y \\ \dot{z} &= V\sin(\gamma) + d_z, \end{aligned} \tag{1}$$

$$\begin{aligned} \dot{V} &= \frac{T-D}{m} - g\sin(\gamma) + d_V \\ \dot{\gamma} &= \frac{g}{V}\left(n\cos(\phi) - \cos(\gamma)\right) + d_\gamma \\ \dot{\psi} &= \frac{L\sin(\phi)}{mV\cos(\gamma)} + d_\psi, \end{aligned} \tag{2}$$

where m is the mass, g is the gravity acceleration, T is the thrust, L is the lift, D is the drag, $n = L/(\mathrm{mg})$ is the g-load and ϕ is the bank angle. The bank angle rotates the lift force in the vertical plane to the correct direction of the side force. The d-components are disturbances in the appropriate directions of the kinematic equations.

The lift and drag forces are often modeled by the relations:

$$D = 0.5\rho\left(V - V_{m,n}\right)^2 S_{Aw} C_{D_0} + \frac{2k_n^2 n^2 m^2}{\rho\left(V - V_m\right)^2 S_{Aw}},$$

where $V_{m,n} = 0.215\ V_m \log_{10}(h) + 0.285\ V_m$, ρ is the atmospheric density, S_{Aw} is the effective wing area, C_{D_0} is the zero-lift drag coefficient, V_m is the mean wind speed at an altitude of h. The drag model contains an algebraic loop which is a fixed-point problem, and was solved approximately in finite steps until a small error is reached. In order to simplify the notations, trigonometrical functions like $\sin(x)$, $\cos(x)$, $\tan(x)$ will be denoted by S_x, C_x, T_x.

2.2 System dynamic equations

The nominal dynamic model can be obtained by taking the first derivative of Eq. (1), which results in:

$$\begin{aligned} \ddot{x} &= \dot{V}C_\psi C_\gamma + V\left(-S_\psi \dot{\psi} C_\gamma - S_\gamma \dot{\gamma} C_\psi\right) + \dot{d}_x \\ \ddot{y} &= \dot{V}S_\psi C_\gamma + V\left(C_\psi \dot{\psi} C_\gamma - S_\psi S_\gamma \dot{\gamma}\right) + \dot{d}_y \\ \ddot{z} &= \dot{V}S_\gamma + VC_\gamma \dot{\gamma} + \dot{d}_z. \end{aligned} \tag{3}$$

Substituting Eq. (2) into Eq. (3), the nominal model with disturbance is obtained in the composite form:

$$\begin{aligned} \dot{p} &= v \\ \dot{v} &= M\xi - N - b + w, \end{aligned} \tag{4}$$

where $\xi = M^{-1}(N + b)$, $\dot{v} = a$ is the acceleration, $b = (0, 0, g)^T$ is the gravity acceleration and w is the disturbance. The control variable is constructed from the components T, n, and ϕ such that $\xi = (T,\ n\cos(\phi),\ L\sin(\phi))^T$ forms the input to the dynamics in Eq. (2). The matrices in Eq. (4) are described as:

$$\begin{aligned} M &= \frac{1}{m}\begin{bmatrix} C_\gamma C_\psi & -mgS_\gamma C_\psi & -S_\psi \\ C_\gamma S_\psi & -mgS_\gamma S_\psi & C_\psi \\ S_\gamma & mgC_\gamma & 0 \end{bmatrix} \\ N &= \frac{1}{m}\begin{bmatrix} DC_\gamma C_\psi \\ DC_\gamma S_\psi \\ DS_\gamma \end{bmatrix} \\ w &= \begin{bmatrix} d_V C_\gamma C_\psi - d_\gamma V S_\gamma C_\psi - d_\psi V C_\gamma S_\psi + \dot{d}_x \\ d_V C_\gamma S_\psi - d_\gamma V S_\gamma S_\psi + d_\psi V C_\gamma S_\psi + \dot{d}_y \\ d_V S_\gamma + d_\gamma V C_\gamma + \dot{d}_y \end{bmatrix}. \end{aligned} \tag{5}$$

2.3 Modeling aerodynamic disturbances

It is assumed that the aerodynamic disturbance effects are proportional with nominal effects and that:

$$\begin{aligned} M^n + M^\Delta &= \left(I_3 + K_1\right)M \\ N^n + N^\Delta &= \left(I_3 + K_2\right)N, \end{aligned} \tag{6}$$

where K_1 and K_2 are diagonal matrices of the model perturbation parameters α. In case of perturbations, the dynamic model can be brought into the composite form:

$$\begin{aligned} \dot{p} &= v \\ \dot{v} &= M\xi - N - b + w + K_1 M\xi - K_2 N \\ &= a + \Omega^{*T}\sigma\left(v\right) - b + w. \end{aligned} \tag{7}$$

The perturbations are chosen as:

$$K_1 M\xi - K_2 N = K_1 M \begin{bmatrix} T \\ nC_\phi \\ LS_\phi \end{bmatrix} - K_2 N. \tag{8}$$

For instance, while considering the second column of matrix M weighted by nC_ϕ, it follows:

$$-mgnC_\phi \begin{bmatrix} S_\gamma C_\psi \\ S_\gamma S_\psi \\ -C_\gamma \end{bmatrix} = -\frac{mg}{V} nC_\phi T_\gamma diag\left(1,1,\frac{-1}{T_\gamma^2}\right)^T \sigma\left(v\right), \tag{9}$$

where $\sigma(v) = (v_x, v_y, v_z)^T$. Therefore, if Eq. (8) is approximated only by the diagonal elements, where $K_1 = K_2 = \alpha$, then:

$$\Omega^{*T} \approx \frac{1}{mV} diag\left(\begin{bmatrix} K_1 T - K_2 D \\ -K_1 mgnC_\phi T_\gamma - K_2 D \\ -K_2 D \end{bmatrix}\right). \tag{10}$$

2.4 Nominal controller design for a single UAV

Since the system dynamic model has a single input, the state feedback design is a simple task that can be solved by using pole placement or linear quadratic regulator control. The goal is to prescribe a Hurwitz matrix and determine the state feedback gain. The state variable is $x = (p^T, v^T)^T$, the high-level control input is the acceleration a, and ξ is the low-level control. From Eq. (7), and using model reference adaptive control principles given in [1], the control design can be summarized as:

$$\begin{aligned} &\dot{x} = Ax + B\left(a + \Omega^{*T}\sigma\left(x\right) - b + w\right) \\ &A_m = A + Bk_1^{*T} \quad \text{Hurwitz} \\ &B_m = Bk_2^{*T} \rightarrow B_m\eta = Bk_2^{*T}\eta \\ &\boldsymbol{B} = B_m\eta\left(k_2^{*T}\eta\right)^{-1} = B_m\left(k_2^{*T}\right)^{-1} \\ &\Gamma = \left(k_2^{*T}\eta\right) = \left(k_2^{*T}\eta\right)^T > 0. \end{aligned} \tag{11}$$

Notice that the system's state equation is a double integrator, and hence, k_1^{*T} makes A_m Hurwitz, and B_m is appropriately chosen. A simple choice is that $\eta = \eta_s I_\eta$ where η_s is a scalar and I_η is a unit matrix. Furthermore, A_m should satisfy the Lyapunov equation $A_m^T P + PA_m = -Q$, for $P > 0$ and $Q > 0$.

3 Stability and parameter tuning in UAV formations

3.1 Signal boundedness in adaptive control

Control inputs are usually based on the appropriately defined and easily computable system errors. Since it is important to assure bounded outputs for bounded inputs, then the system error too should be bounded. A possible way is to introduce a dead zone function $\mu\left(\|e\|\right)$ to suppress parameter tuning of small errors, and to limit the tuning above a certain threshold, say e_0.

3.2 Relations between stability and parameter tuning

Important results given in [21] for Lipschitz-continuous projection operator are presented to aid in formulation of the control laws. Let $J(\theta)$: $R^n \rightarrow R$ be a convex differentiable function, $\nabla J(\theta)$ is its gradient vector, and define the following sets: $\Omega_0 = \{\theta : J(\theta) \leq 0\}$ and $\Omega_1 = \{\theta : J(\theta) \leq 1\}$ for all t. Suppose that the parameter vector θ^* belongs to the set Ω_0, then the projection operator is defined as in [21]:

$$\text{Proj}\left(\theta, y\right) = y - \frac{\Gamma\nabla J\left(\theta\right)\left(\nabla J\left(\theta\right)\right)^T}{\left\|J\left(\theta\right)\right\|_\Gamma^2} yJ\left(\theta\right), \tag{12}$$

for $J\left(\theta\right) > 0 \wedge y^T\nabla J\left(\theta\right) > 0,$ otherwise Proj(θ, y) = y. Then for any positive definite matrix Γ, it yields the relation:

$$\left(\theta - \theta^*\right)\left(\Gamma^{-1}\text{Proj}\left(\theta, \Gamma y\right) - y\right) \leq 0. \tag{13}$$

The following result [22] is of conceptual importance for parameter tuning in adaptive controllers satisfying $\dot{\theta} = \text{Proj}\left(\theta, y\right)$. Starting from an initial condition $\theta\left(0\right) = \theta_0 \in \Omega_0,$ the parameter trajectory will remain in Ω_1 for all time $t > 0$. For matrix parameter Θ, the projection operator is extended as $\dot{\Theta} = \text{Proj}\left(\Theta, \Gamma\right)$. In this sense, in the convex inequality for stability, the projection operator is extended as:

$$\text{Proj}\left(\Theta, \Gamma Y\right) = \left(\text{Proj}\left(\theta_1, \Gamma y_1\right),\ \ldots,\ \text{Proj}\left(\theta_n, \Gamma y_n\right)\right). \tag{14}$$

Let the control signal be $u = -\Theta^T\Phi(x)$ for a Hurwitz A_m. The parameter estimation error is then defined as $\tilde{\Theta} = \hat{\Theta} - \Theta$, and the error differential equation with a bounded disturbance is described as:

$$\dot{e} = A_m - B\tilde{\Theta}^T\Phi(x) + d(t), \quad \|d(t)\| \le d_{\max}, \tag{15}$$

where e represents a local tracking error. A candidate radially bounded quadratic Lyapunov function, $V(e,\tilde{\Theta})$ is chosen in the form:

$$V(e,\tilde{\Theta}) = e^T Pe + \text{trace}\left(\tilde{\Theta}^T\Gamma_\Theta^{-1}\tilde{\Theta}\right), \tag{16}$$

and the time derivative is given as:

$$\begin{aligned}\dot{V} &= -e^T Qe + 2\text{trace}\left(\tilde{\Theta}^T\left(\Gamma_\Theta^{-1}\dot{\tilde{\Theta}} - \Phi e^T PB\right)\right)\\ &+2e^T Pd(t) \le -\lambda_{\max}(Q)\|e\|^2 + 2\|e\|\lambda_{\max}(P)d_{\max},\end{aligned} \tag{17}$$

where the trace term is simplified using the relation:

$$\begin{aligned}&\text{trace}\left(\tilde{\Theta}^T\left(\Gamma^{-1}\text{Proj}(\hat{\Theta},\Gamma Y) - Y\right)\right) \le 0\\ &\Rightarrow \text{trace}(*) = \sum\tilde{\Theta}_j^T\left(\Gamma^{-1}\text{Proj}\left(\hat{\Theta}_j,\Gamma Y_j\right) - Y_j\right) \le 0.\end{aligned}$$

Making in Eq. (17) the term inside the trace to be equal to zero, an adaptation law in Eq. (18) is arrived at where $\Gamma_\Theta > 0$ is positive definite weight, $\Phi(x)$ is weighting matrix, e is the error vector, P and B were described previously.

$$\dot{\hat{\Theta}} = \Gamma_\Theta\Phi(x)e^T PB \tag{18}$$

However, $\dot{V}(e,\tilde{\Theta}) < 0$ yields outside the compact set:

$$E_0 = \left\{(e,\tilde{\Theta}) : \|e\| \le 2\frac{\lambda_{\max}(P)}{\lambda_{\min}(Q)}d_{\max} = e_0\right\}. \tag{19}$$

According to [22], trajectories $e(t)$ of the error dynamics enter in finite time into a compact set $\Omega_0 \supset E_0$, i.e., Ω_0 contains E_0, and will remain there in the $(e,\tilde{\Theta})$ space. Notice that the inequality Eq. (17) can be written in the form:

$$\dot{V}(e,\tilde{\Theta}) \le -\lambda_{\min}(Q)\|e\|\left(\|e\| - 2\frac{\lambda_{\max}(P)d_{\max}}{\lambda_{\min}(Q)}\right).$$

Hence, $\dot{V}(e,\tilde{\Theta}) < 0$ yields outside the compact set:

$$\begin{aligned}\Omega &= \left\{(e,\tilde{\Theta}) : \|e\| \le 2\frac{\lambda_{\max}(P)}{\lambda_{\max}(Q)}d_{\max} \wedge \|\tilde{\Theta}\|_F \tilde{\Theta}_{\max}\right\}\\ \tilde{\Theta}_{\max} &= 2\left(\Theta_{1,\max},\ldots,\Theta_{m,\max}\right) = 2\Theta_{\max},\end{aligned} \tag{20}$$

where $\Theta_{j,\max}$ is the maximum allowable bound for the j-th column of $\hat{\Theta}(t)$. It is evident that assuring bounded parameters can support the boundedness of signals.

A very simple consequence for a first order scalar actuator model $\tau\dot{u} = u_{cmd} - u$, where u_{cmd} is a reference signal of the actuator, is if $|u| \le u_{\max}$ for a first order has to be satisfied then a function:

$$J(u) = \left((1+\varepsilon)u^2 - u_{\max}^2\right)/\left(\varepsilon u_{\max}^2\right)$$

can assure that the conditions about the compact set Ω_0 are equivalent to $|u| \le u_{\max}/\sqrt{1+\varepsilon}$ and that for Ω_1 then the condition is equivalent to $|u| \le u_{\max}$. Hence, starting with conservative limits $\pm u_{\max}/\sqrt{1+\varepsilon}$, the actuator position will not exceed the preset limits $\pm u_{\max}$.

4 Design of the control algorithm

The formation is assumed to be composed of homogenous UAVs, whose topology is described using a directed graph with tree structure [23]. The formation is a distance consensus-based formation defined by a constant offset vector $\delta_{p,i}$. Therefore, there exists p_0 and v_0 such that $p_i(t) - \delta_{p,i} - p_0(t) \to 0$ and $v_i(t) - v_0(t) \to 0$ as $t \to \infty$ and consequently, $((\delta_{p,i} - \delta_{p,j})^T, 0^T)^T =: \Delta_i - \Delta_j = \Delta_{ij}$. The position and velocity of the i^{th} UAV are $p_i(t)$ and $v_i(t)$ respectively, $p_i(\infty) - p_0(\infty) = \delta_{p,i}$, $v_i(\infty) = v_0(\infty)$ and Δ_{ij} is a constant.

The local tracking error is then defined as:

$$e_i = x_i - \Delta_i - \frac{1}{n_i}\sum_{j\in N_i}\left(x_j - \Delta_j\right) = \frac{1}{n_i}\sum_{j\in N_i}\left(x_i - x_j - \Delta_{ij}\right), \tag{21}$$

where the set N_i and the number n_i are determined from the directed graph. If the local tracking error satisfies $\lim_{t\to\infty} e_i(t) = 0$ then the global tracking error $x_i(t) - x_0(t)$ satisfies:

$$\lim_{t\to\infty}\left(x_i(t) - x_0(t)\right) = \Delta_i + \frac{1}{n}\sum_k\Delta_k \quad \text{for } i = 1,\ldots,n. \tag{22}$$

This result is based on [1, 24]. Notice that Eq. (22) is equivalent to the consensus state $\Delta_0 = -(1/n)\sum_k\Delta_k$ by defining a central location for the virtual leader in the formation.

The global tracking error definition together with the choice of Δ_0, while representing $d_i = -b_i + w_i$, results in the following relationships:

$$\begin{aligned}\dot{x}_0 &= Ax_0 + Bu_0\\ \dot{x}_i &= Ax_i + B\left(u_i + f_i(x_i) + d_i\right)\\ \dot{x}_j &= Ax_j + Bu_j,\end{aligned} \tag{23}$$

$$\begin{aligned}\dot{x}_i - \dot{x}_0 &= A\left(x_i - x_0 - \Delta_i - \frac{1}{n}\sum_k\Delta_k\right)\\ &+B\left(u_i - u_0 + f_i(x_i) + d_i\right)\\ \dot{x}_j - \dot{x}_0 &= A\left(x_j - x_0 - \Delta_j - \frac{1}{n}\sum_k\Delta_k\right) + B\left(u_j - u_0\right)\\ \dot{e}_i &= \frac{1}{n_i}\sum_{j\in N_i}\left(\dot{x}_i - \dot{x}_j\right).\end{aligned} \tag{24}$$

The time derivative of the error can be expanded as:

$$\begin{aligned}\dot{e}_i &= \dot{x}_i - \dot{x}_j \\ &= A\left(x_i - x_j\right) + B\left(u_j + \Omega_i^{*T}\sigma\left(x_i\right) + d_i - \frac{1}{n_i}\sum_{j\in N_i} u_j\right) \\ &= Ae_i + B\left(u_i - \frac{1}{n_i}\sum_{j\in N_i} u_j + \Omega_i^{*T}\sigma\left(x_i\right) + d_i\right).\end{aligned} \tag{25}$$

Using these relationships, a distributed model reference adaptive control [2] as postulated for multi-agent systems in [8], is given as:

$$u_i^a = \frac{1}{n_i}\sum_{j\in N_i}\left(\hat{k}_{1ij}^T\left(x_i - x_j - \Delta_{ij}\right) + u_j\right) - \hat{\Omega}_i^T\sigma_i\left(x_i\right), \tag{26}$$

and with the inclusion of an integral term W_i, for suppressing disturbances, it is written as:

$$\begin{aligned}u_i = &\frac{1}{n_i}\sum_{j\in N_i}\left(\hat{k}_{1ij}^T\left(x_i - x_j - \Delta_{ij}\right) + u_j\right) - \hat{\Omega}_i^T\sigma_i\left(x_i\right) \\ &- \frac{W_i^2 k_2^{*-T} B_m^T P e_i}{W_i + a_i^{-t}},\end{aligned} \tag{27}$$

where $W_i = \tau_i\int_0^t \left\| e_i^T P B_m k_2^{*-1}\right\|^2 dt,$ and the parameter tuning rules are defined from Eq. (18) as:

$$\dot{\hat{k}}_{1ij}^T = \mathrm{Proj}\left(\hat{k}_{1ij}^T, -\frac{1}{n_i}\eta^T B_m^T P \mu\left(\left\|e_i\right\|\right) e_i\left(x_i - x_j - \Delta_{ij}\right)^T\right), \tag{28}$$

$$\dot{\hat{\Omega}}_i^T = \mathrm{Proj}\left(\hat{\Omega}_i^T, \eta^T B_m^T P \mu\left(\left\|e_i\right\|\right) e_i \sigma_i^T\left(x_i\right)\right). \tag{29}$$

The control law u_i reveals that for consensus-based formation, the state $x_j \in N_i$ and the control u_j of the neighbors are necessary. Substituting Eq. (27) into Eq. (25) and making the necessary substitutions of the Eq. (11), while denoting the estimation errors as $\tilde{\Omega}_i^T = \hat{\Omega}_i^T - \Omega_i^{*T}$, one can obtain the global error differential equation as:

$$\begin{aligned}\dot{e}_i = &A_m e_i + B_m k_2^{*-1}\left(\frac{1}{n_i}\sum_{j\in N_i}\left(\tilde{k}_{1ij}^T\left(x_i - x_j - \Delta_{ij}\right)\right)\right) \\ &+ B_m k_2^{*-1}\left(-\tilde{\Omega}_i^T\sigma_i\left(x_i\right) + d_i - \frac{W_1^2 k_2^{*-T} B_m^T P e_i}{W_i + a_i^{-t}}\right).\end{aligned} \tag{30}$$

The control algorithm utilizes the local errors Eq. (21), and the adaptive gains $\hat{k}_{1ij}^T$, and $\hat{\Omega}_i^T$, and the error integral W_i.

5 Simulation results

To verify the performance of the proposed control algorithm, four homogenous fixed wing UAV vehicles were used in the simulations. Fig. 1 describes the directed graph topology of the fixed wing UAVs with respect to the virtual leader, represented as 0.

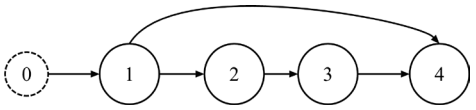

Fig. 1 Directed graph topology of the UAV swarm

The desired separation distances $\delta_p = (\delta_{p,1}, \delta_{p,2}, \delta_{p,3}, \delta_{p,4})$ between the UAVs and the virtual leader are set as given in Table 1.

The weight of each UAV is m_i = 20 kg and the gravitational acceleration was taken as g = 9.81 m/s^2. The other model parameters are $C_{D_0} = 0.02,$ wing area S_{Aw} = 1.37 m^2, dynamic pressure ρ = 1.225 kg/m^3, $k_n = 1, k_d = 0.1, V_m = 4$ m/s.

The initial states of the UAVs were taken as $V_i(0)$ = (70, 60, 40, 50) m/s, $\gamma_i(0)$ = 0 rad, and ψ_i = 0 rad. The starting positions of each vehicle is given in Table 2.

Parameters of the controller were set as Q = [1, 0; 0, 1], η = 0.01, $\Gamma = 0.5 \times 10^{-3}$, $k_2^* = 0.005,$ δ = 0.01. The closed loop poles were placed at $eig = (-2, -1)^T$, and the matrices A_m, B_m, P, and e_0 were computed as discussed previously. The projection bound is set as $\theta_m = 1$ and tolerance as $\varepsilon_\theta = 0.1$. Table 3 shows the tunable parameters for the formation control algorithm, where 'X' means that the parameter is adaptively tuned. The set of tunable parameter options can be selected and activated in various combinations.

5.1 Formation control simulation in nominal case

In this simulation experiment, it was assumed that there are neither disturbances nor model perturbations present

Table 1 Desired formation distance configuration

$\delta_{p,i}$	Distance
1	(0, 100, 0)
2	(−100, 0, 0)
3	(0, −100, 0)
4	(100, 0, 0)

Table 2 Initial UAV position states

UAV	Position (x, y, z)
1	(0, 200, 95)
2	(0, 60, 90)
3	(0, −200, 70)
4	(0, −60, 80)

Table 3 Set of tunable parameters

	W_i	k_{1ij}^T	$\hat{\Omega}_i^T$
Nominal	–	X	X
Disturbed case without tuning	X	–	–
Disturbed case with tuning	X	X	X

affecting the system, and the feedback gain computed from the placement of the desired closed loops $k_{1ij}^T = (-2,-3)^T$ is a matrix of appropriate dimension.

Fig. 2 shows the trajectories of the UAVs' position in 3D space, and their convergence to the desired formation topology. Fig. 3 shows the corresponding position tracking errors, and the velocity tracking errors are shown in Fig. 4. The tracking errors converge to zero after about 5 s, and this represents the control time for the UAVs to converge to the desired formation.

In Fig. 5, the evolution of the model parameters is shown where it can be observed that the velocity, V_i of all the UAVs converges to that preset for the virtual leader of 60 m/s, and the model angles γ and ψ converge to zero radians respectively. The control input for each vehicle is shown in Fig. 6.

5.2 Disturbed case without tuning

In this simulation experiment, the system was subjected to external disturbances and parameter perturbations. The disturbances affecting each of the vehicles are approximated using bounded continuous-time functions and their values are given in Table 4.

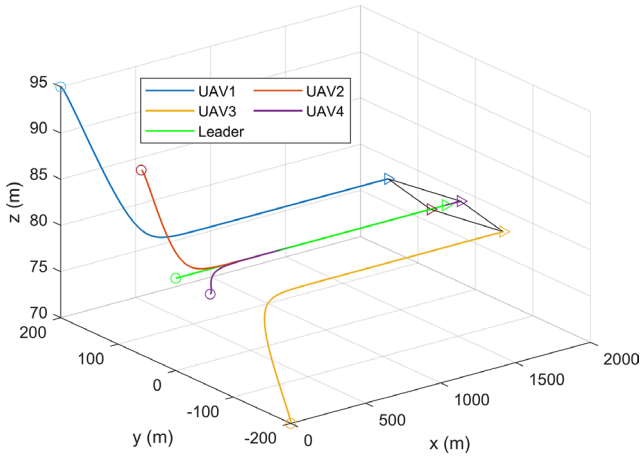

Fig. 2 3D position trajectories of the UAVs

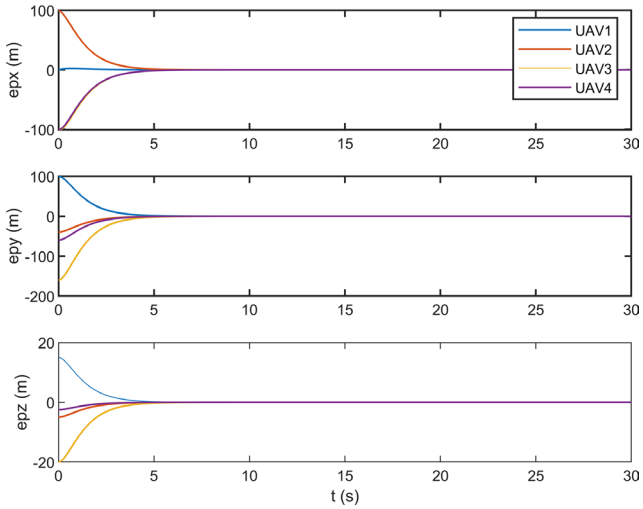

Fig. 3 Position tracking errors

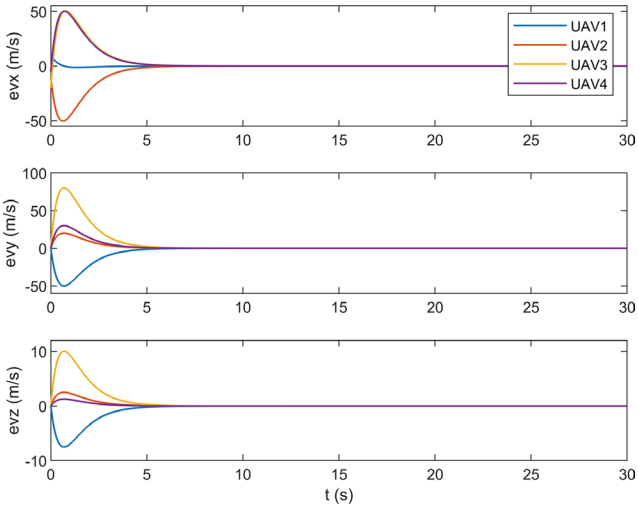

Fig. 4 Velocity tracking errors

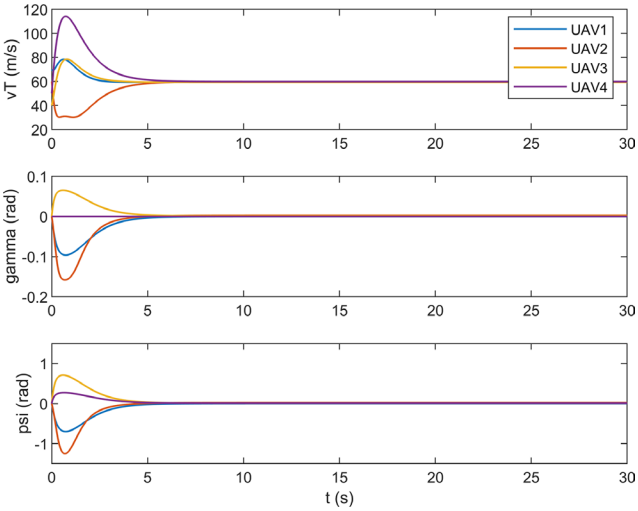

Fig. 5 Evolution of model parameters

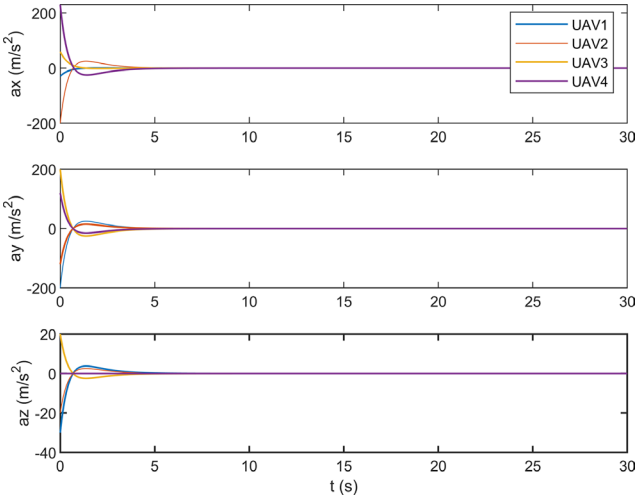

Fig. 6 Acceleration level input

Table 4 External disturbances

UAV	$d_{(x,y,z)}$	$d_{(V,\gamma,\psi)}$
1	$(2C_t, 1.5C_t, -0.5C_t)$	$(1.5S_t, 0.8C_t, 0.8C_t)$
2	$(2S_t, 3S_t, -S_t)$	$(2S_t, 0.75S_t, 0.75S_t)$
3	$(3C_t, C_t, -C_t)$	$(3S_t, 0.5C_t, 0.5C_t)$
4	$(1.5S_t, 2S_t, -0.5S_t)$	(S_t, C_t, C_t)

The model perturbation parameters, α were set as α_i = (0.15, 0.10, −0.15, 0.10) where negative value imply the parameter is less than the nominal value as specified. The nominal control was used as in the previous case.

The numerical simulation results are shown in Figs. 7 to 11. The 3D positions trajectories in Fig. 7 show the convergence of the vehicles to the desired formation, in spite of the disturbed dynamics. The position and velocity tracking errors shown in Fig. 8 and Fig. 9 are almost convergent with small perturbations noticed along the z axis.

The evolution of the dynamic parameters is not convergent as seen in Fig. 10 however, the effect of the disturbances

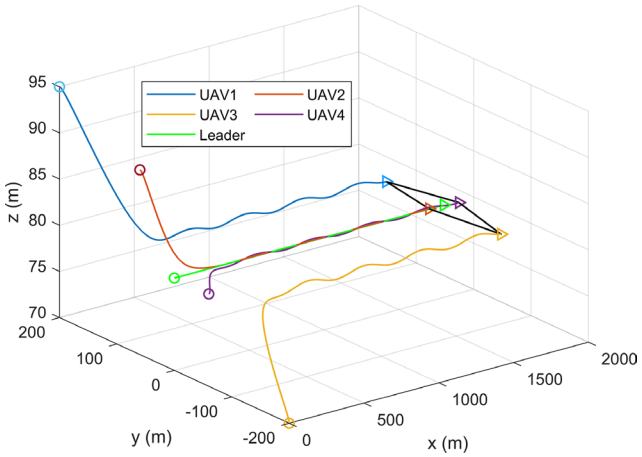

Fig. 7 3D position trajectories in this scenario

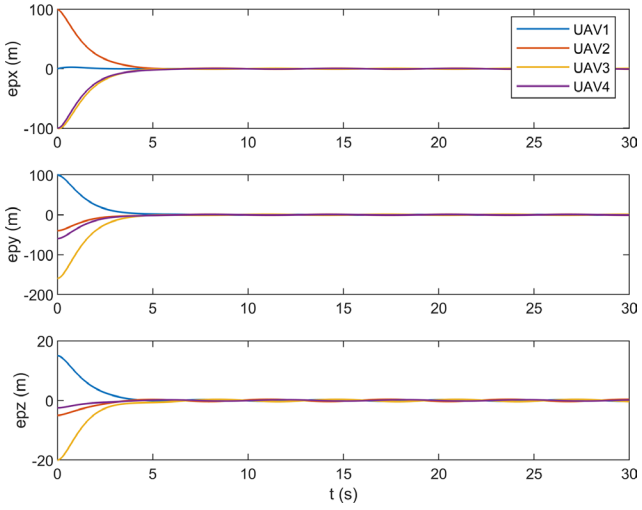

Fig. 8 Position tracking errors

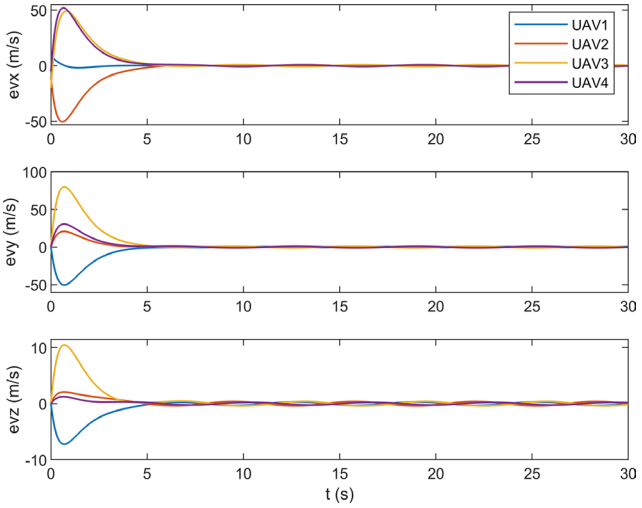

Fig. 9 Velocity tracking errors

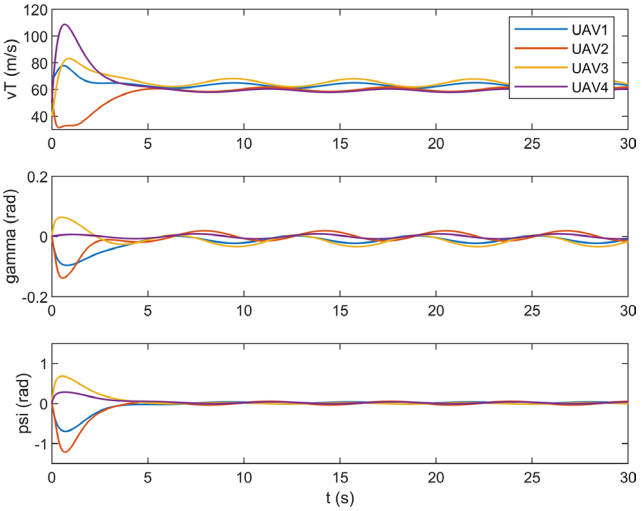

Fig. 10 Parameter trajectories of the dynamic model

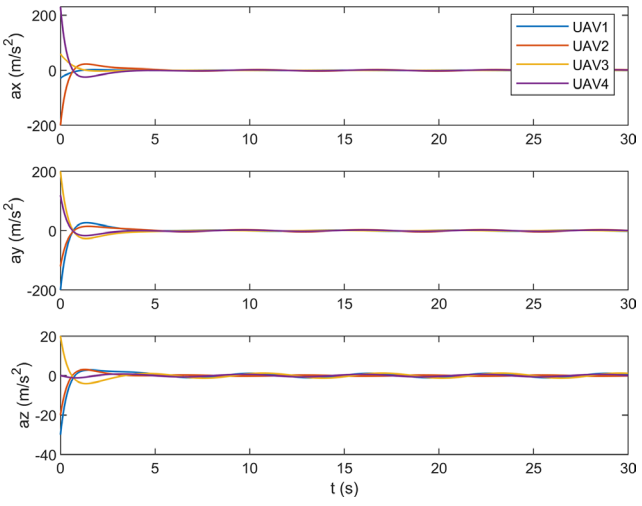

Fig. 11 Acceleration control input

and uncertainties are bounded. The acceleration level input is shown in Fig. 11. This experiment shows that the nominal control based on model reference adaptive control was

able to uniformly bound the disturbances, while still steer the vehicles to converge the desired formation shape.

5.3 Disturbed case with tuning

The control law used is that in Eq. (27), with the tuning of the adaptive parameters k_{1ij}^T and $\hat{\Omega}_i^T$ using Eq. (28) and Eq. (29), and the parameters of the embedded feedback error integral were set as $\tau_i = (0.3, 0.4, 0.2, 0.5)$, and $a = 2$.

The position trajectories are shown in Fig. 12, and the tracking errors are shown in Fig. 13 and Fig. 14 respectively. Due to the presence of tuning of the parameters, and the inclusion of the feedback error integral term, there was a significant reduction of the perturbations on the system kinematics. The evolution of parameter adaptation of k_{1ij}^T and $\hat{\Omega}_i^T$ are shown in Fig. 15 and Fig. 16 respectively, and all settle to constant values.

The evolution of the dynamic parameters is shown in Fig. 17. The dynamic parameters settle within an acceptable steady-state range. The control variable for the formation

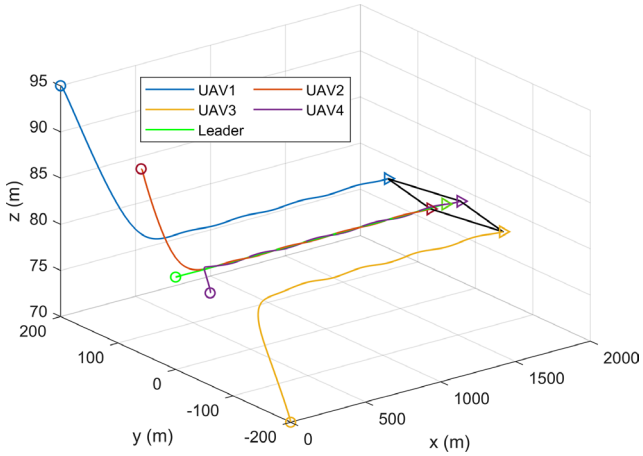

Fig. 12 3D position trajectories in this scenario

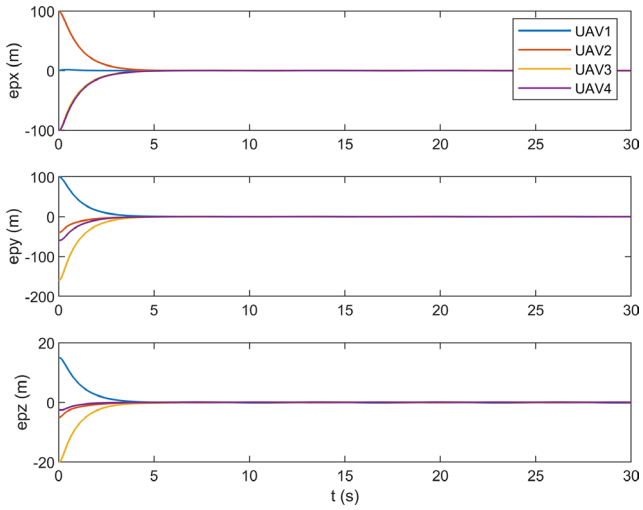

Fig. 13 Position tracking errors

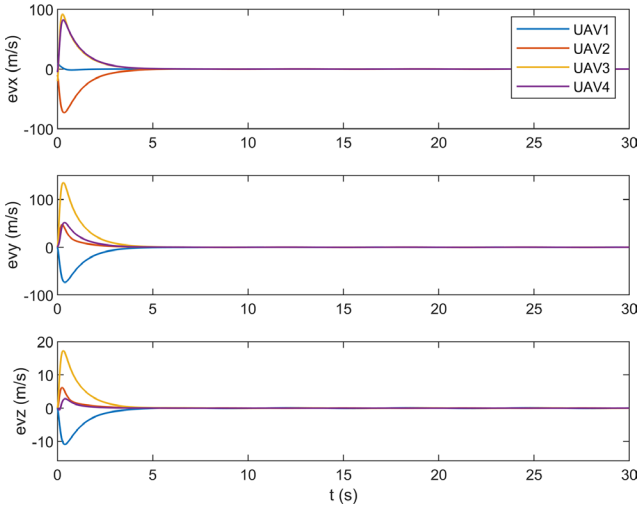

Fig. 14 Velocity tracking errors

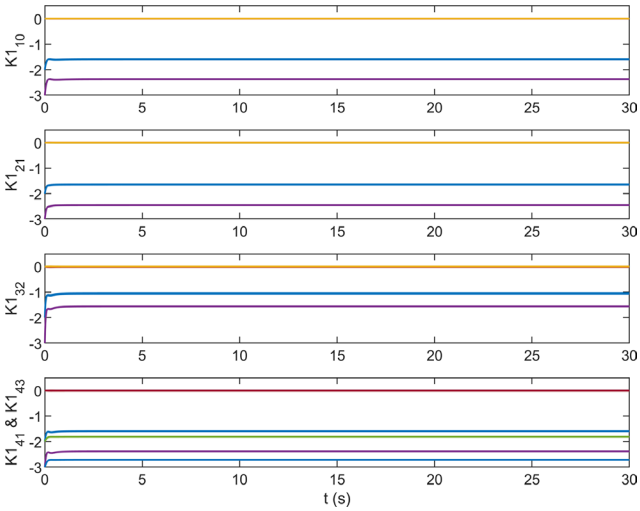

Fig. 15 Adaptive formation gains

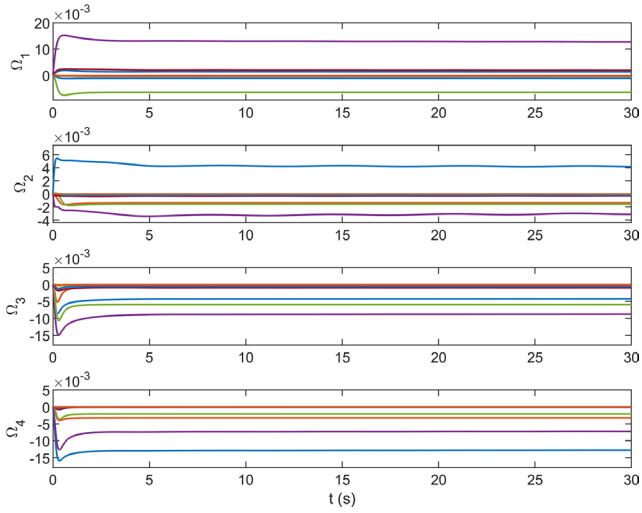

Fig. 16 Adaptive estimate of parameter uncertainties

tracking is shown in Fig. 18. The acceleration level system control input is high due to the integral action, but still fits into theoretical bounds associated with flight control; these

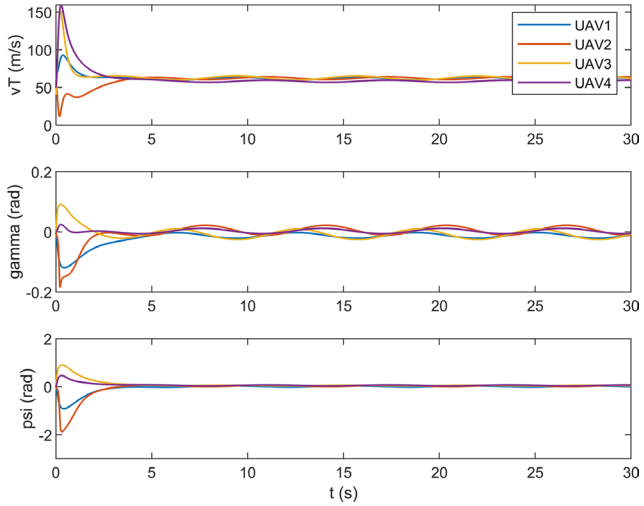

Fig. 17 Evolution of the dynamic model parameters

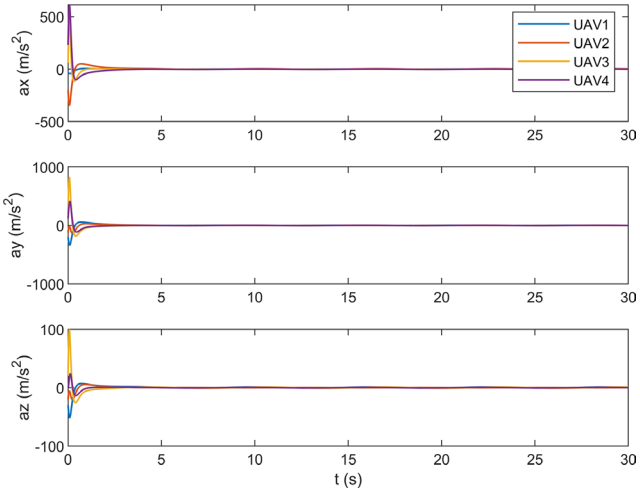

Fig. 18 Acceleration control input

values should not be confused with the vehicle's accelerations, which are the time derivatives of body velocities.

Although the dynamics parameters do not accurately settle to those of the virtual leader, the kinematic errors head to zero. We have demonstrated that the control strategy bounds the states of the system, and performs well in forming and maintaining the prescribed formation shape of the UAVs even under the presence of disturbances, and parameter variations affecting the vehicles.

6 Conclusion

This paper has presented the formation control of fixed wing unmanned aerial vehicles based on the distributed model reference adaptive control. Consensus-based principles were applied to stabilize the multi-agent vehicle system in the presence of unstable double integrator dynamics. Due to this, an initial stabilization was done using state feedback. Simulation results presented show the effectiveness of the proposed control strategy to form and maintain a prescribed formation during tracking of the group's reference trajectory. The inclusion of an integral error control component dependent on the tracking errors guaranteed an improved suppression of the disturbances effect on the formation system.

References

[1] Lavretsky, E., Wise, K. A. "Robust and Adaptive Control: With Aerospace Applications", Springer-Verlag London, 2013. ISBN 978-1-4471-4396-3
https://doi.org/10.1007/978-1-4471-4396-3

[2] Zhi, Y., Liu, L., Guan, B., Wang, B, Cheng, Z., Fun, H. "Distributed robust adaptive formation control of fixed-wing UAVs with unknown uncertainties and disturbances", Aerospace Science and Technology, 126, 107600, 2022.
https://doi.org/10.1016/j.ast.2022.107600

[3] Liang, Y., Dong, Q., Zhao, Y. "Adaptive leader–follower formation control for swarms of unmanned aerial vehicles with motion constraints and unknown disturbances", Chinese Journal of Aeronautics, 33(11), pp. 2972–2988, 2020.
https://doi.org/10.1016/j.cja.2020.03.020

[4] Yu, Y., Chen, J., Zheng, Z., Yuan, J. "Distributed Finite-Time ESO-Based Consensus Control for Multiple Fixed-Wing UAVs Subjected to External Disturbances", Drones, 8(6), 260, 2024.
https://doi.org/10.3390/drones8060260

[5] Imran, I. H., Kurtulus, D. F., Memon, A. M., Goli, S., Kouser, T., Alhems, L. M. "Distributed Robust Formation Control of Heterogeneous Multi-UAVs With Disturbance Rejection", IEEE Access, 12, pp. 55326–55341, 2024.
https://doi.org/10.1109/access.2024.3390183

[6] Wang, J., Wang, C., Wei, Y., Zhang, C. "Bounded neural adaptive formation control of multiple underactuated AUVs under uncertain dynamics", ISA Transactions, 105, pp. 111–119, 2020.
https://doi.org/10.1016/j.isatra.2020.06.002

[7] Peng, Z., Wang, D., Zhang, H., Sun, G., Wang, H. "Distributed model reference adaptive control for cooperative tracking of uncertain dynamical multi-agent systems", IET Control Theory & Applications, 7(8), pp. 1079–1087, 2013.
https://doi.org/10.1049/iet-cta.2012.0765

[8] Goel, R., Roy, S. B. "Closed-loop Reference Model based Distributed Model Reference Adaptive Control for Multi-agent Systems", In: 2021 American Control Conference (ACC), New Orleans, LA, USA, 2013, pp. 1082–1087. ISBN 978-1-7281-9704-3
https://doi.org/10.23919/ACC50511.2021.9483063

[9] Su, Y. H., Bhowmick, P., Lanzon, A. "A robust adaptive formation control methodology for networked multi-UAV systems with applications to cooperative payload transportation", Control Engineering Practice, 138, 105608, 2023. https://doi.org/10.1016/j.conengprac.2023.105608

[10] Prayitno, A., Nilkhamhang, I. "Distributed Model Reference Adaptive Control for Vehicle Platoons with Uncertain Dynamics", Engineering Journal, 25(8), pp. 173–185, 2021. https://doi.org/10.4186/ej.2021.25.8.173

[11] Xi, J., Yao, Z., Liu, G., Zhong, Y. "Swarm stability for high-order linear time-invariant singular multi-agent systems", International Journal of Systems Science, 46(8), pp. 1458–1471, 2015. https://doi.org/10.1080/00207721.2013.822610

[12] Kladis, G. P., Menon, P. P., Edwards, C. "Cooperative tracking for a swarm of Unmanned Aerial Vehicles: A distributed Tagaki-Sugeno fuzzy framework design", In: 2011 50th IEEE Conference on Decision and Control and European Control Conference, Orlando, FL, USA, 2011, pp. 4114–4119. ISBN 978-1-61284-800-6 https://doi.org/10.1109/CDC.2011.6161123

[13] Wang, F., Gao, Y., Zhou, C., Zong, Q. "Disturbance observer-based backstepping formation control of multiple quadrotors with asymmetric output error constraints", Applied Mathematics and Computation, 415, 126693, 2022. https://doi.org/10.1016/j.amc.2021.126693

[14] Xiao, H., Li, Z., Chen, C. L. P. "Formation Control of Leader–Follower Mobile Robots' Systems Using Model Predictive Control Based on Neural-Dynamic Optimization", IEEE Transactions on Industrial Electronics, 63(9), pp. 5752–5762, 2016. https://doi.org/10.1109/TIE.2016.2542788

[15] Yamchi, M. H., Esfanjani, R. M. "Distributed predictive formation control of networked mobile robots subject to communication delay", Robotics and Autonomous Systems, 91, pp. 194–207, 2017. https://doi.org/10.1016/j.robot.2017.01.005

[16] Chen, W., Hua, S., Ge, S. S. "Consensus-based distributed cooperative learning control for a group of discrete-time nonlinear multi-agent systems using neural networks", Automatica, 50(9), pp. 2254–2268, 2014. https://doi.org/10.1016/j.automatica.2014.07.020

[17] Zou, A.-M., Kumar, K. D. "Neural network-based adaptive output feedback formation control for multi-agent systems", Nonlinear Dynamics, 70(2), pp. 1283–1296, 2012. https://doi.org/10.1007/s11071-012-0533-9

[18] Zhen, Z., Tao, G., Xu, Y., Song, G. "Multivariable adaptive control based consensus flight control system for UAVs formation", Aerospace Science and Technology, 93, 105336, 2019. https://doi.org/10.1016/j.ast.2019.105336

[19] Rodrigues, J., Figueira, D., Neves, C., Ribeiro, I. "Leader-Following Graph-Based Distributed Formation Control", In: Proceedings of Robotica'2008, Bali, Indonesia, 2008, pp. 71–77. ISBN 978-972-96895-3-6

[20] Wang, J., Xin, M. "Integrated Optimal Formation Control of Multiple Unmanned Aerial Vehicles", IEEE Transactions on Control System Technology, 21(5), pp. 1731–1744, 2013. https://doi.org/10.1109/TCST.2012.2218815

[21] Lavretsky, E., Gibson, T. E., Annaswamy, A. M. "Projection Operator in Adaptive Systems", [preprint] arXiv, arXiv:1112.4232v6, 16 October 2012. https://doi.org/10.48550/arXiv.1112.4232

[22] Khalil, H. K. "Nonlinear Systems", Prentice Hall, 2002. ISBN 0-13-067389-7

[23] Xu, Y., Zhen, Z. "Multivariable adaptive distributed leader-follower flight control for multiple UAVs formation", The Aeronautical Journal, 121(1241), pp. 877–900, 2017. https://doi.org/10.1017/aer.2017.42

[24] Song, G. "Adaptive Control of Distributed Leader-Follower Consensus of Multiagent Systems", PhD Thesis, University of Virginia, 2015.